Biuletyn WAT
Vol. LXVII, Nr 3, 2018

Dynamic displacement analysis of reinforced concrete deep beams made of high strength concrete

Part III: Analysis of dynamic displacement of a reinforced concrete deep beam made of high strength *C300* grade concrete

WALDEMAR CICHORSKI

Military University of Technology, Faculty of Civil Engineering and Geodesy,
2 Gen. W. Urbanowicza Str., 00-908 Warsaw, Poland, waldemar.cichorski@wat.edu.pl

Abstract. This work demonstrates an analysis of the displacement state of rectangular concrete deep beams made of very high strength concrete grade *C300* under a dynamic load, including the physical nonlinearity of construction materials: concrete and reinforcing steel. The analysis was conducted with the method presented in [1]. Numerical solution results are presented with particular reference to the displacement state of a rectangular concrete deep beam. The work confirmed the accuracy of the assumptions and deformation models of concrete and steel as well as the effectiveness of the methods of analysis proposed in the paper [1] for the problems of numerical simulation of the behaviour of reinforced concrete deep beams under dynamic loads. A comparative analysis was conducted on the effect of the high-strength concrete and the steel of increased strength on the displacement of a grade *C300* concrete deep beam vs. the results produced in [10] for grade *C100* and *C200* concrete deep beams.
Keywords: mechanics of structures, reinforced concrete structures, deep beams, dynamic load, physical nonlinearity
DOI: 10.5604/01.3001.0012.6610

1. Introduction

The purpose of this work was to analyse the effects of very high-strength concrete and increased-strength reinforcing steel on the displacement of rectangular reinforced-concrete deep beams under dynamic loads and with consideration of physical non-linearity of concrete and reinforcing steel, the construction materials.

The assumptions adopted for structural modelling of the construction materials and the solution method are explained in Part One of this work, [10]. The subject of this analysis, the geometric features of the deep beams, the material parameters of the concrete and of the reinforcing steel, and the estimation of static carrying capacity levels of specific deep beam types, as determined per [9], are also shown in Part One, [10]. The considerations presented in this work are based on an analysis of deformation of rectangular deep beams made from grade *C300* concrete and reinforced with regular reinforcing steel in one version and with increased-strength reinforcing steel in another version. The comparative analysis of the results included the results from the analysis of effort of the reinforced concrete deep beam made with grade *C100* concrete, presented in [10], and with grade *C200* concrete, presented in [11].

2. Analysis of numerical results

To illustrate the effect of very high-strength concrete on the displacement state of rectangular reinforced concrete deep beams, numerical experiments were carried out on the deep beam with the reinforcement arranged as in the experiment [6] and with modified parameters describing the constitutive concrete model (in this part, concrete

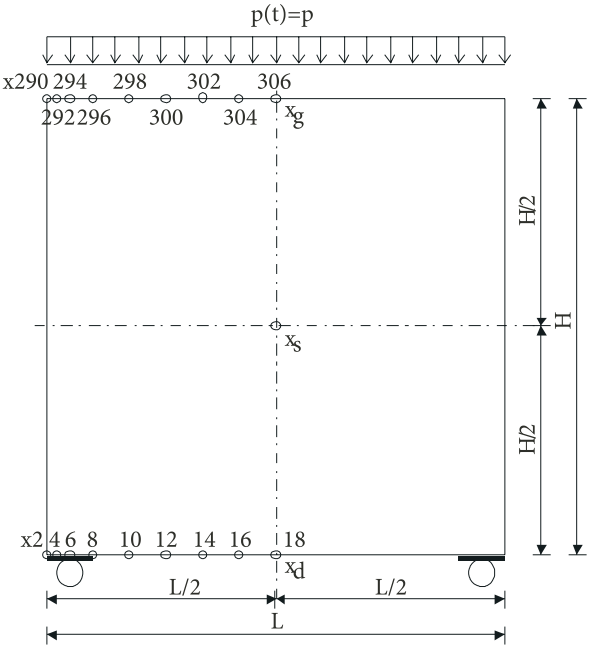

Fig. 1. Location of the points for displacement observation

grade *C300* was used). Additionally, the effect of changing the strength parameters of reinforcing steel, i.e. the influence of replacing grade *A-III* regular steel, the one used in the experiment [6], with increased-strength steel (grade *A-H*), was analysed.

For that purpose, the following points in the central section (designated in Fig. 1) were adopted for the observation of dynamic changes of displacement of the deep beam: x_d — on the lower edge, x_s — in the centre of the deep beam height, x_g — on the upper edge. In turn, the following points were selected for the observation in order to illustrate the variability over time of the lower and upper edge of the deep beam:

— on the lower edge of the deep beam: x_2, x_4, x_6, x_8, x_{10}, x_{12}, x_{14}, x_{16}, x_{18};
— on the upper edge of the deep beam: x_{290}, x_{292}, x_{294}, x_{296}, x_{298}, x_{300}, x_{302}, x_{304}, x_{306};

the locations of which are show in Fig. 1.

2.1. Reinforced-concrete deep beam reinforced with regular steel (A-III)

Fig. 2 shows the variability of vertical displacement over time of selected points in the central section at various load levels $\alpha = P/P_0$. At the load level $\alpha = 0.3$, Fig. 2_1, in the elastic range and with a minor level of inelastic processes in the concrete, the results revealed a relation between the vertical displacements similar to that found in the deep beams made from grade *C100* and *C200* concrete: $v(x_g) > v(x_s) > v(x_d)$. As the load was increased to $\alpha = 0.4$, Fig. 2_2, the vertical displacement of lower point x_d increased just like in the deep beams made from grade *C100* and *C200* concrete: Because of the cracks (scratching) of the concrete in the lower layers of the shear zone, a partial modification of the interrelation of the changes of individual vertical displacements over time: $v(x_g) > v(x_d) \cong v(x_s)$. As the load was increased to $\alpha = 0.5$, Fig. 2_3, the propagation of the crack areas occurred only in part of the crack area extent found in the *C200* concrete deep beam in that the propagation was only observed in the upward vertical direction in the shear zone only. An effect of this was not unlike in the *C200* concrete deep beam: it did not modify the interrelation of the changes of individual vertical displacements over time, i.e. $v(x_g) > v(x_d) \cong v(x_s)$. At the load level of $\alpha = 0.6$, Fig. 2_4 (not unlike in the *C100* and *C200* concrete deep beams), a lack of stabilisation of plastic processes was observed and manifested with a stabilized vibrating movement around the permanent displacements of the observed points at lower load levels. However, the process of vibration movement stability loss at this load level was distributed over time and progressed differently than in the *C100* and *C200* concrete deep beams. As an effect of the development of the concrete crack zones in one area, diagonally from the shear zone with upward vertical propagation, the carrying capacity of the deep beam was lost.

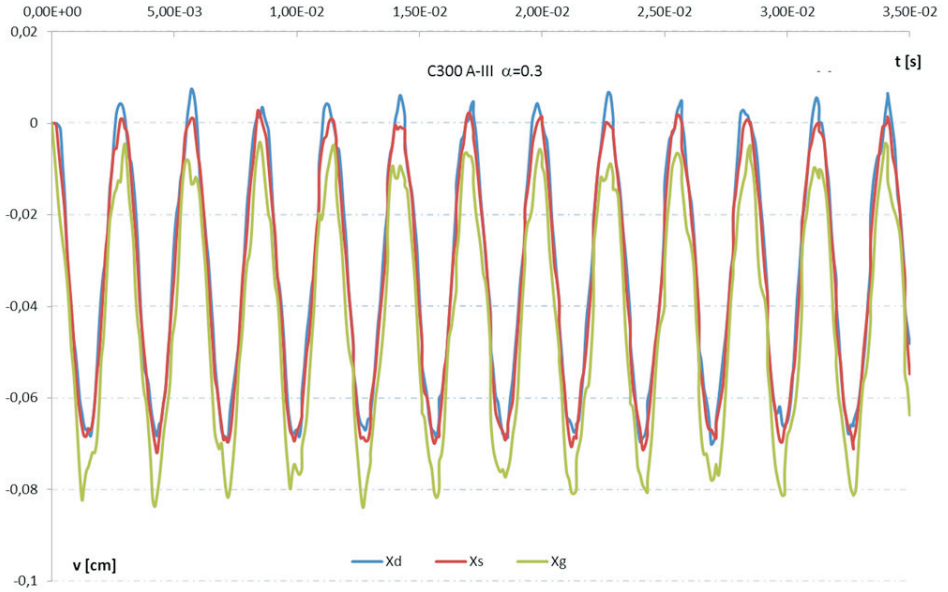

Fig. 2_1. Change of vertical displacements over time of the points in the central section at the load level $\alpha = 0.3$

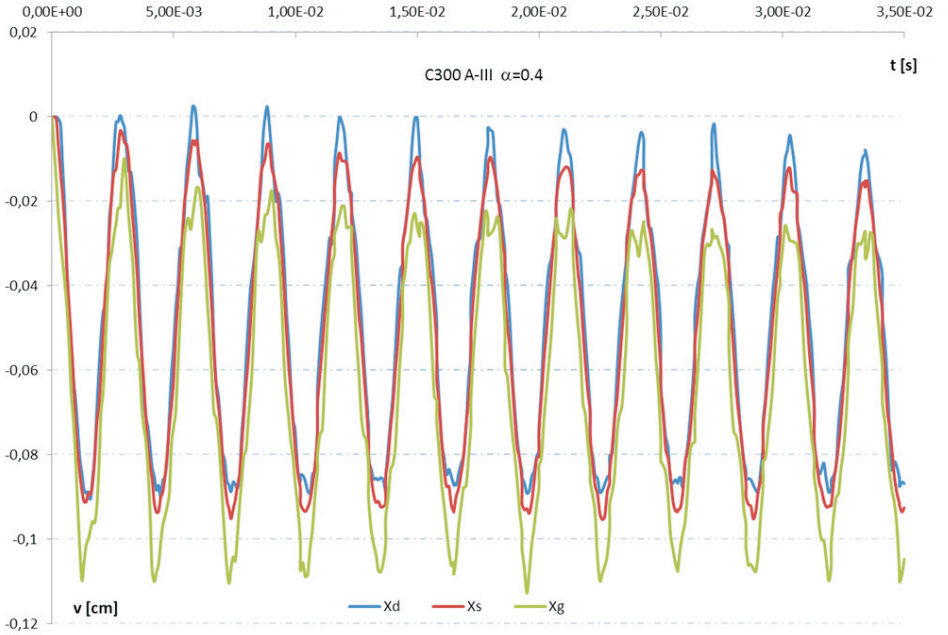

Fig. 2_2. Change of vertical displacements over time of the points in the central section at the load level $\alpha = 0.4$

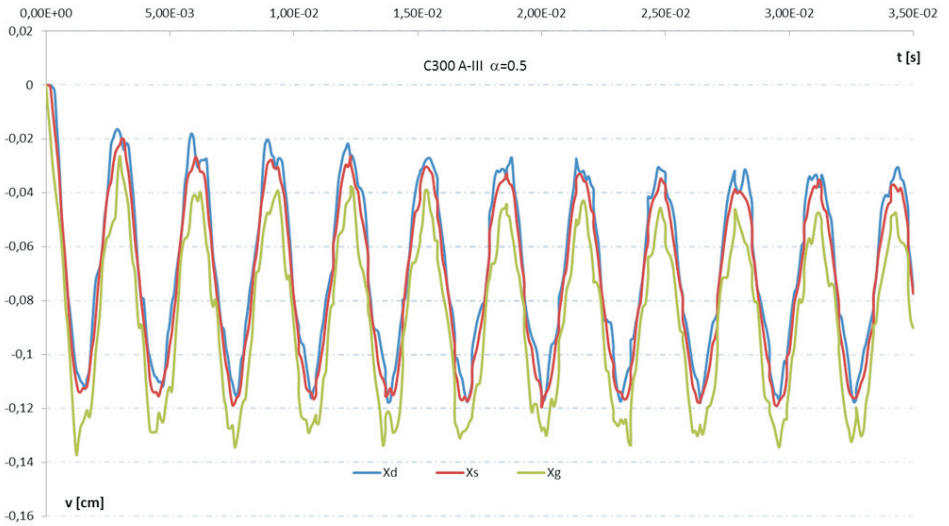

Fig. 2$_3$. Change of vertical displacements over time of the points in the central section at the load level $\alpha = 0.5$

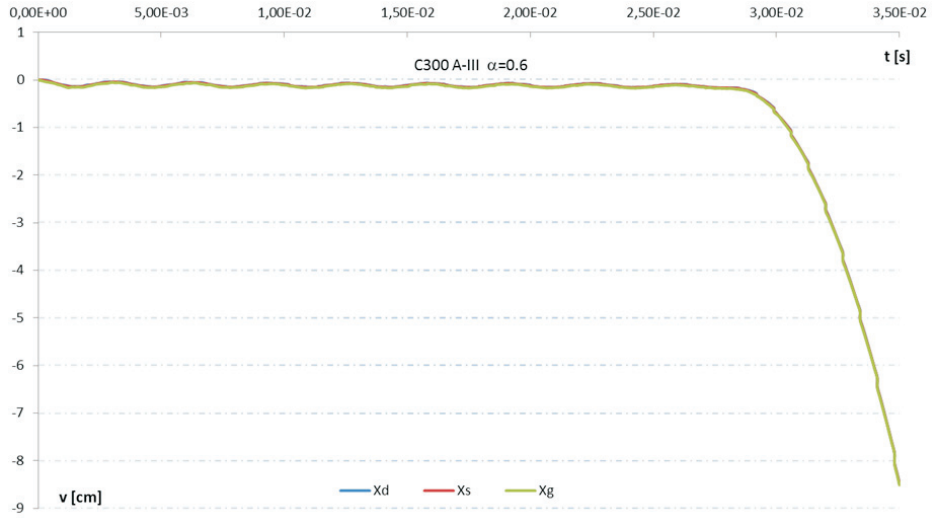

Fig. 2$_4$. Change of vertical displacements over time of the points in the central section at the load level $\alpha = 0.6$

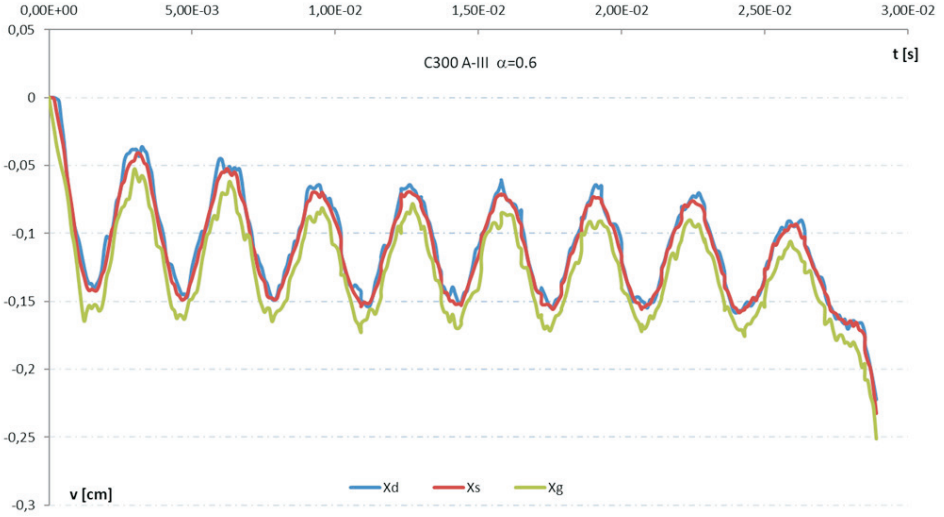

Fig. 2_{4a}. Change of vertical displacements over time of the points in central section at the load level α = 0.6 — detail of Fig. 2_4 (with a reduced time interval of the analysis)

Fig. 3 shows the variability of the vertical displacement over time of the selected points in the lower edge of the deep beam at different load levels $\alpha = P/P_0$. In the range of elastic capacity of the structure, the load $\alpha = 0.1$ and $\alpha = 0.2$ gave the maximum deflection, just like in the *C100* and *C200* concrete deep beams' span at point x_{18}, and the observed amplitude values of the vertical displacements decreased monotonously towards the support. The same behaviour of the structure was observed at the load level $\alpha = 0.3$, (Fig. 3_1), when the cracking of the concrete in proximity of the support occurred. At the load level $\alpha = 0.4$, (Fig. 3_2) and $\alpha = 0.5$, (Fig. 3_3), and similar to the *C200* concrete deep beam, the previous relation was observed: the maximum deflection was at point x_{18} of the span at lower load levels, and the observed amplitudes of vertical displacements decreased monotonously towards the support. At the load level $\alpha = 0.5$, no concrete cracks were found in the central section, unlike in the *C100* concrete deep beam. In Fig. 3_4, which shows the load level $\alpha = 0.6$, further development of the concrete cracking area is found. There was an unlimited increase of vertical displacements at the points adjacent to the span cross-section and indicative of the carrying capacity limit with a failure of the deep beam, just like in the *C200* concrete deep beam.

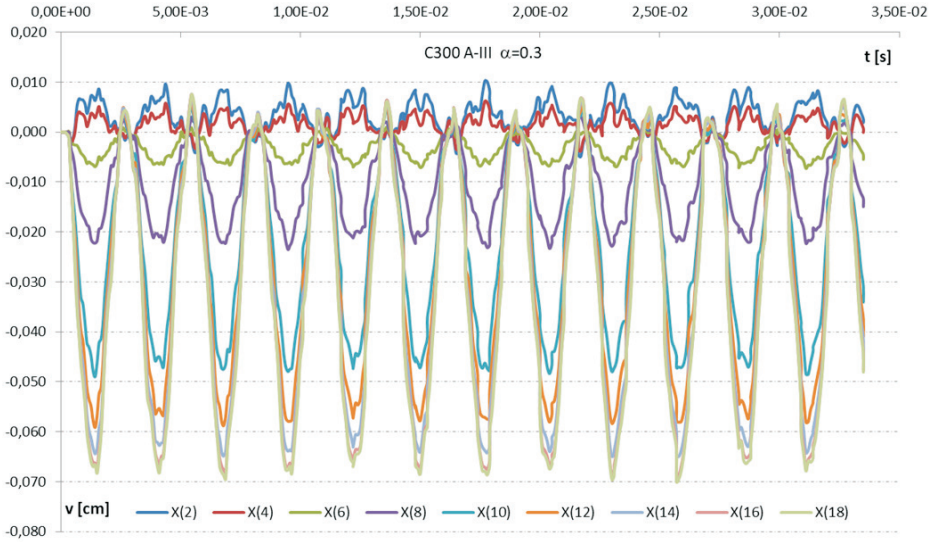

Fig. 3_1. Change of vertical displacements over time of the points in the lower edge of the deep beam at the load level $\alpha = 0.3$

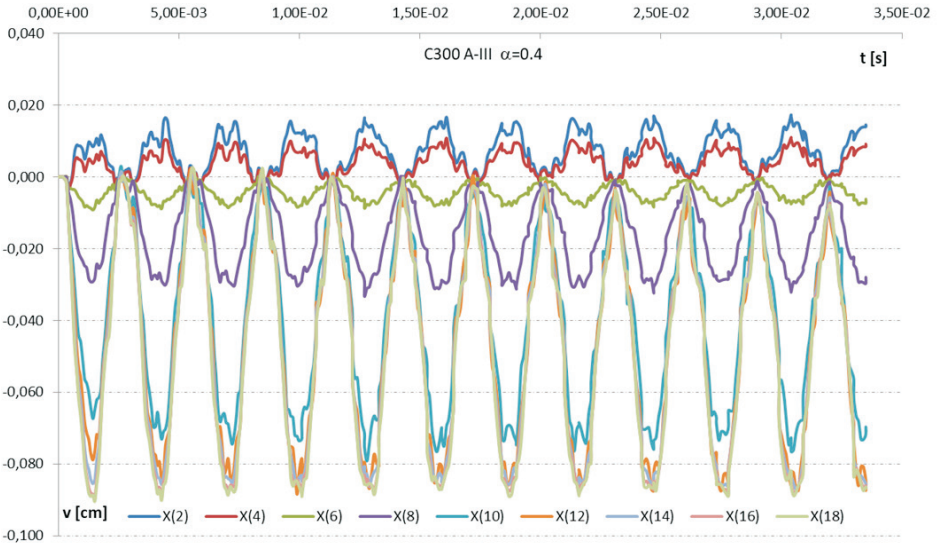

Fig. 3_2. Change of vertical displacements over time of the points in the lower edge of the deep beam at the load level $\alpha = 0.4$

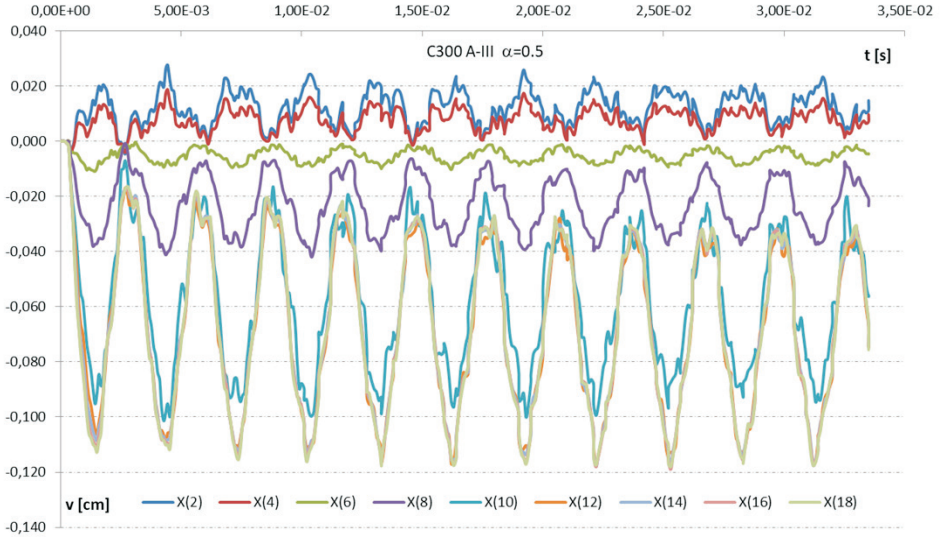

Fig. 3_3. Change of vertical displacements over time of the points in the lower edge of the deep beam at the load level $\alpha = 0.5$

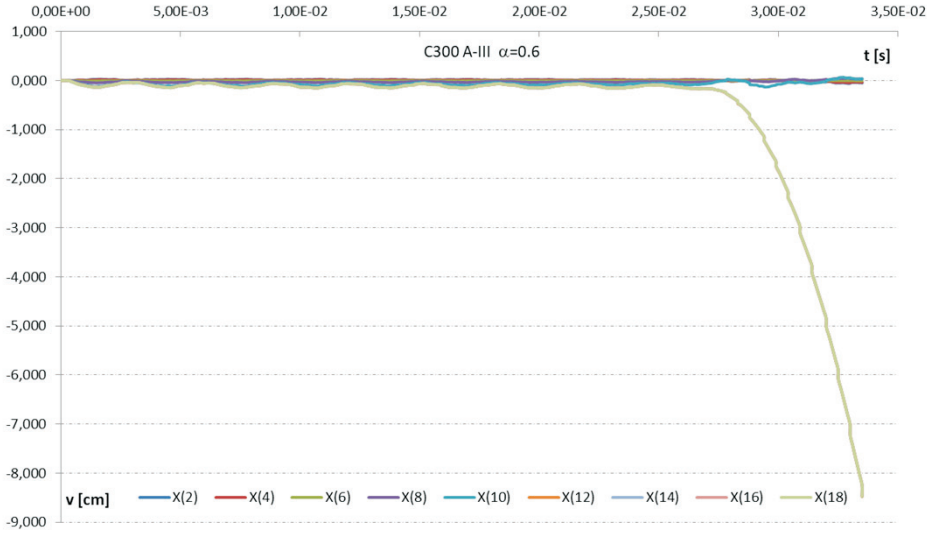

Fig. 3_4. Change of vertical displacements over time of the points in the lower edge of the deep beam at the load level $\alpha = 0.6$

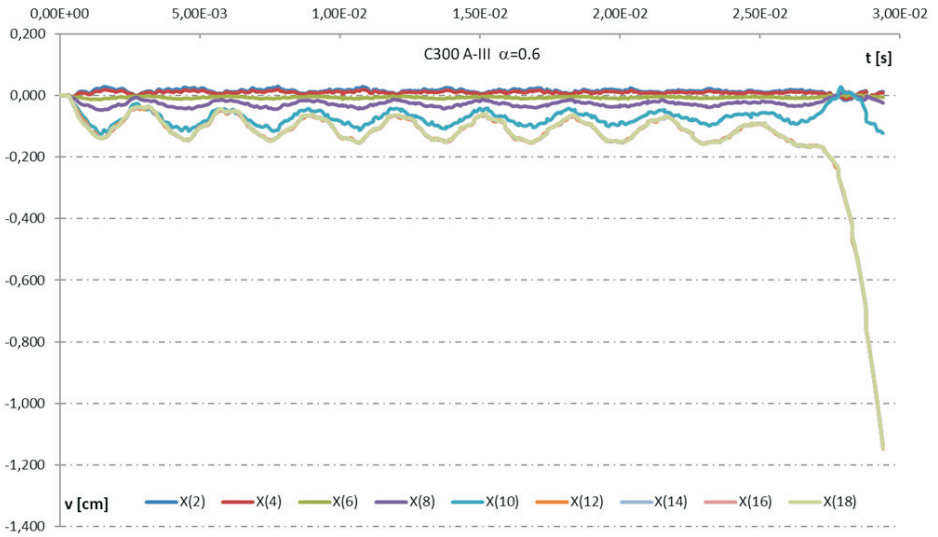

Fig. 3_{4a}. Change of vertical displacements over time of the points in the lower edge of the deep beam at the load level $\alpha = 0.6$ — detail of Fig. 3_4 (with a reduced time interval of the analysis)

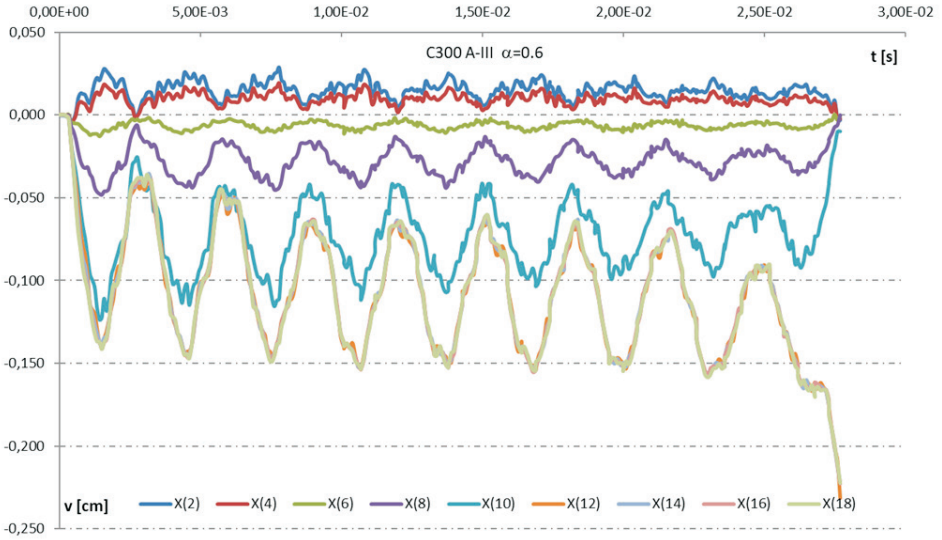

Fig. 3_{4b}. Change of vertical displacements over time of the points in the lower edge of the deep beam at the load level $\alpha = 0.6$ — detail of Fig. 3_4 (with a reduced time interval of the analysis)

Fig. 4 shows the variability of the vertical displacement over time at the selected points in the upper edge of the deep beam at different load levels $\alpha = P/P_0$. At the load levels $\alpha = 0.1$, $\alpha = 0.2$, $\alpha = 0.3$ (Fig. 4_1) and $\alpha = 0.4$, (Fig. 4_2), the maximum deflection was at point x_{306} of the span, just like in the *C100* and *C200* concrete deep beams, and the observed amplitude values of the vertical displacements decreased monotonously towards the support. The same behaviour of the structure, not unlike in the *C200* concrete deep beam, was observed at the load level $\alpha = 0.5$, (Fig. 4_3); however, unlike in the *C100* concrete deep beam, there was no evidence of dynamic balance differentiation, i.e. no permanent displacement of the points on the upper edge occurred. In Fig. 4_4, which shows the load level $\alpha = 0.6$, further development of the concrete cracking area is found. There was an unlimited increase of vertical displacements at the points in the of the central section, i.e. at points x_{306}, x_{304}, x_{302} and x_{300}, indicative of the carrying capacity limit with a failure of the deep beam.

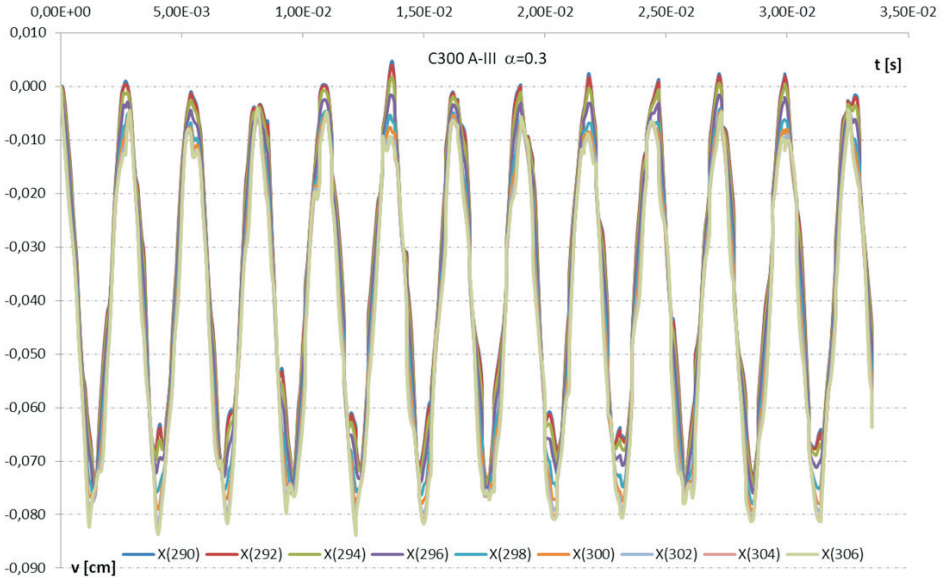

Fig. 4_1. Change of vertical displacements over time of the points in the upper edge of the deep beam at the load level $\alpha = 0.3$

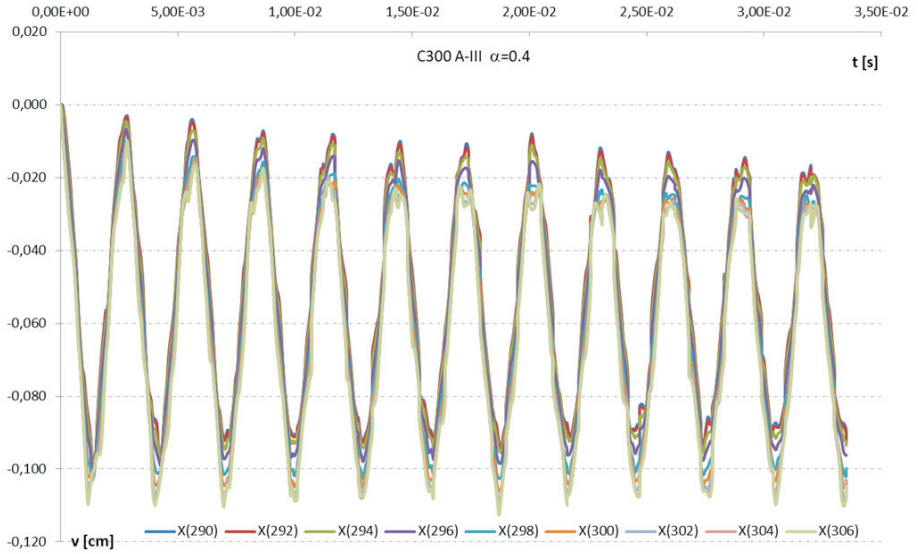

Fig. 4_2. Change of vertical displacements over time of the points in the upper edge of the deep beam at the load level $\alpha = 0.4$

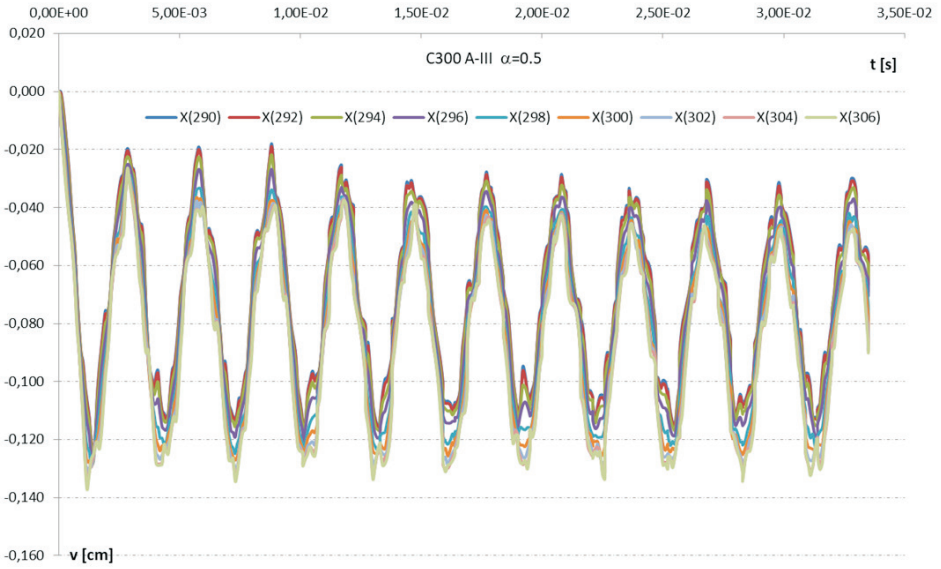

Fig. 4_3. Change of vertical displacements over time of the points in the upper edge of the deep beam at the load level $\alpha = 0.5$

Fig. 4_4. Change of vertical displacements over time of the points in the upper edge of the deep beam at the load level $\alpha = 0.6$

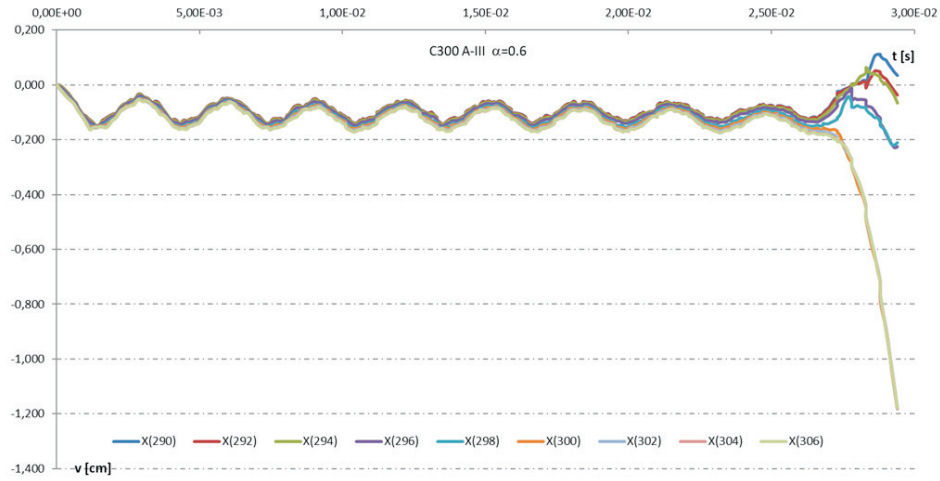

Fig. 4_{4a}. Change of vertical displacements over time of the points in the upper edge of the deep beam at the load level $\alpha = 0.6$ — detail of Fig. 4_4 (with a reduced time interval of analysis)

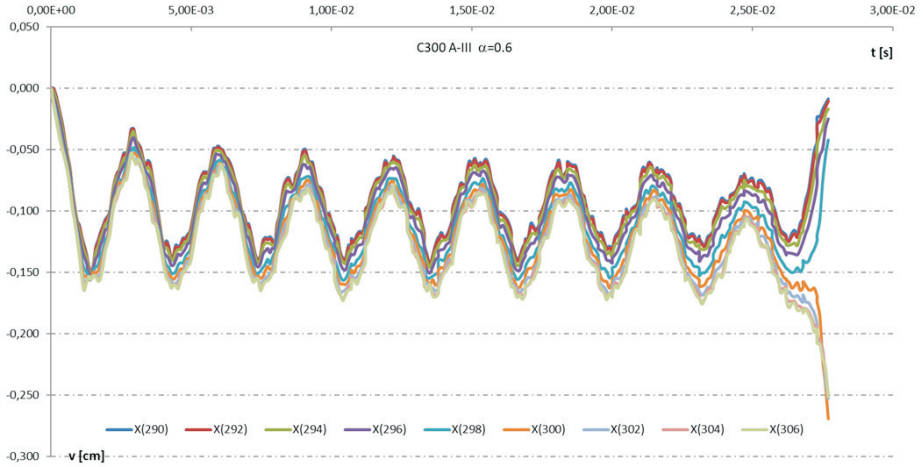

Fig. 4_{4b}. Change of vertical displacements over time of the points in the upper edge of the deep beam at the load level $\alpha = 0.6$ — detail of Fig. 4_{4a} (with a reduced time interval of analysis)

2.2. Reinforced-concrete deep beam reinforced with regular steel (A-H)

Fig. 5 shows the variability of vertical displacement over time of selected points in the central section at various load levels $\alpha = P/P_0$. Up to the load level $\alpha = 0.3$ (Fig. 5_1 and Fig. 5_2), not unlike in a reinforced concrete deep beam with *A-III* reinforcing steel, the structure reacted in the elastic range at a low level of plastic processes in the concrete; the results indicated a known relation between the vertical displacements: $v(x_g) > v(x_s) > v(x_d)$. As the load was increased to $\alpha = 0.4$, Fig. 5_3, the vertical displacement of lower point x_d increased just like in the deep beams reinforced with *A-III* steel. Because of the cracks (scratching) of the concrete in the lower layers of the shear zone, a partial modification of the interrelation of the changes of individual vertical displacements over time: $v(x_g) > v(x_d) \cong v(x_s)$. As the load was increased to $\alpha = 0.5$, Fig. 5_4, the propagation of the crack areas occurred only in part of the crack area extent found in the *A-III* steel reinforced deep beam in that the propagation was only observed in the upward vertical direction in the shear zone only. An effect of this was not unlike in the *A-III* steel reinforced deep beam: it did not modify the interrelation of the changes of individual vertical displacements over time, i.e. $v(x_g) > v(x_d) \cong v(x_s)$. At the load level of $\alpha = 0.6$, Fig. 5_5, not unlike in the *A-III* steel reinforced deep beams, a lack of stabilisation of plastic processes was observed and manifested with a stabilized vibrating movement around the permanent displacements of the observed points at lower load levels. However, the process of vibrating motion stability loss was more violent in the deep beam reinforced with *A-III* steel.

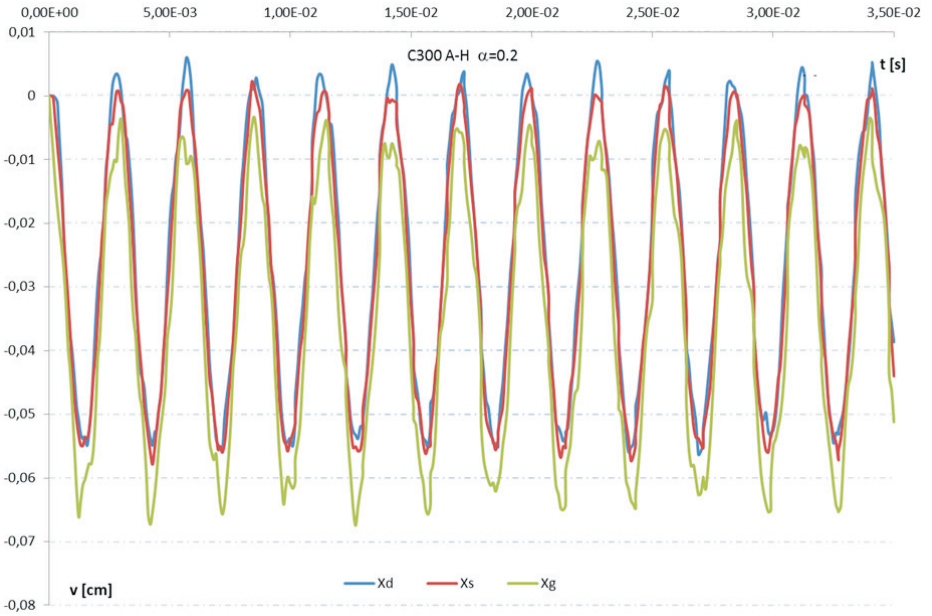

Fig. 5_1. Change of vertical displacements over time of the points in the central section at the load level $\alpha = 0.2$

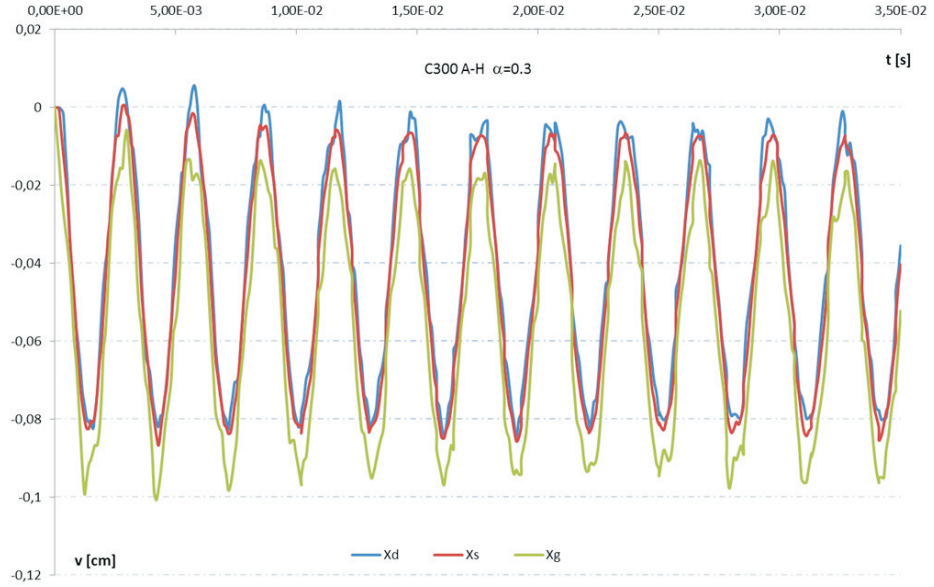

Fig. 5_2. Change of vertical displacements over time of the points in the central section at the load level $\alpha = 0.3$

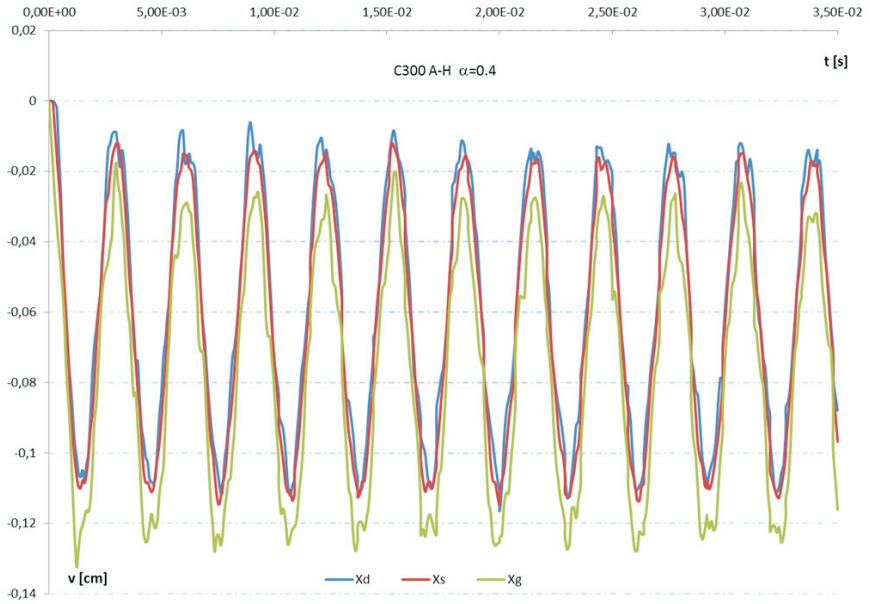

Fig. 5_3. Change of vertical displacements over time of the points in the central section at the load level $\alpha = 0.4$

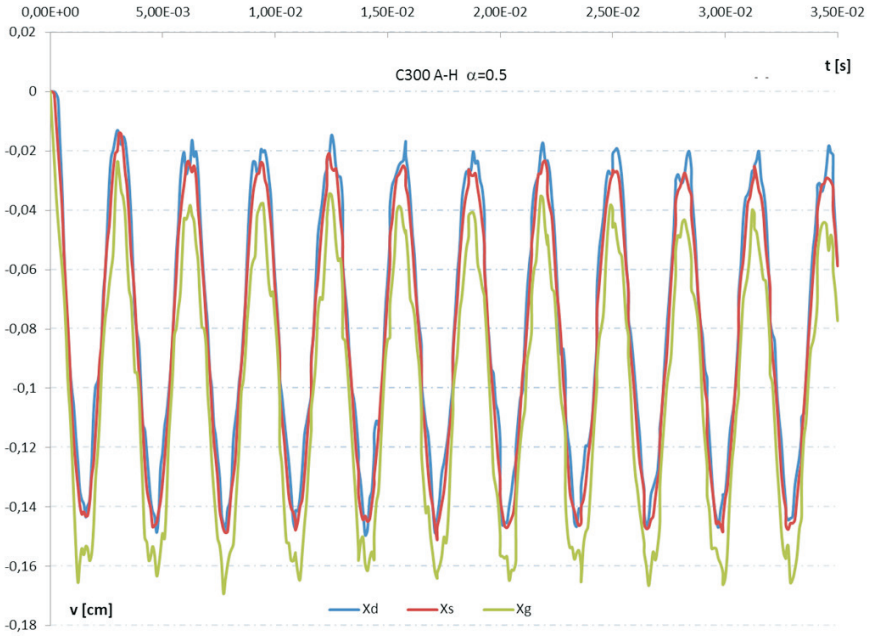

Fig. 5_4. Change of vertical displacements over time of the points in the central section at the load level $\alpha = 0.5$

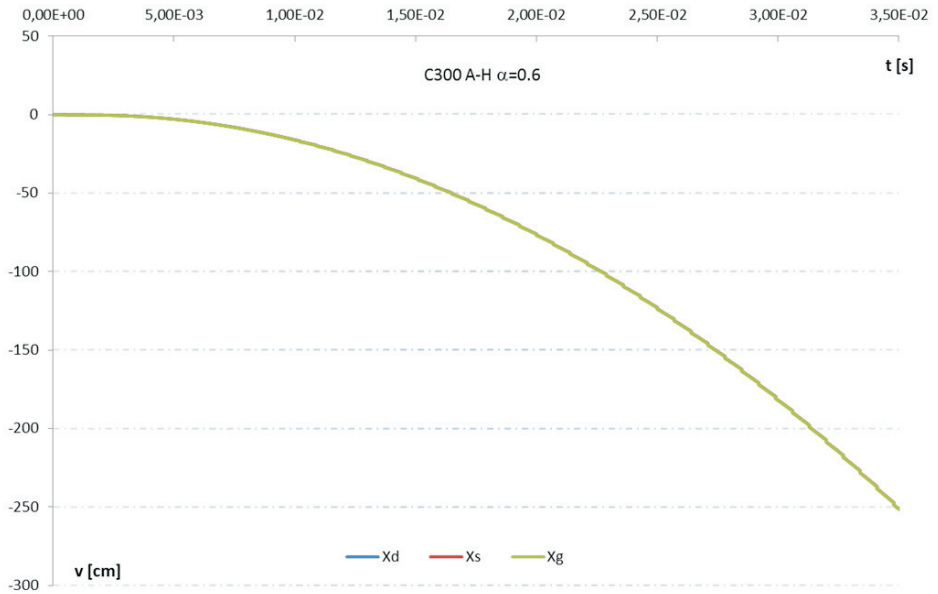

Fig. 5_5. Change of vertical displacements over time of the points in the central section at the load level $\alpha = 0.6$

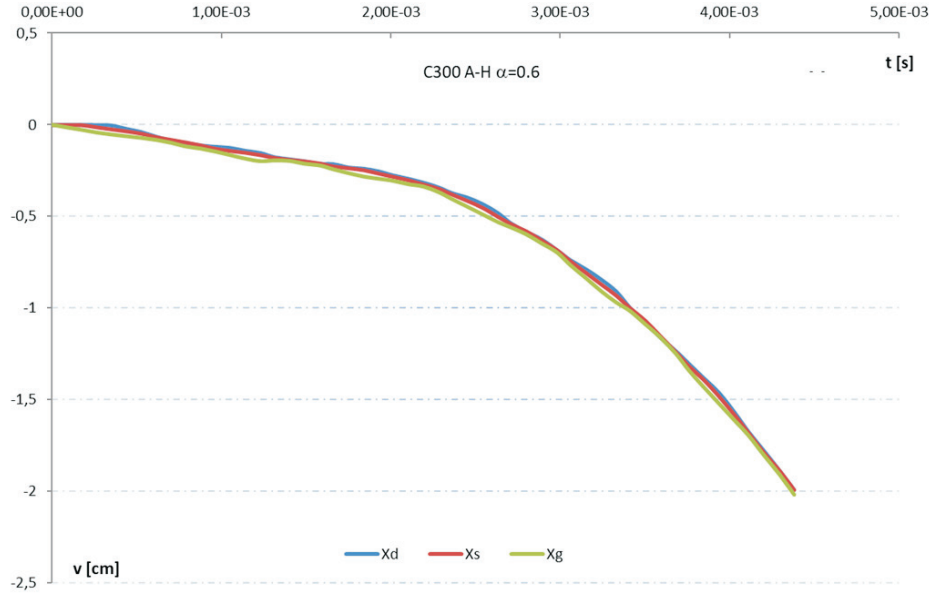

Fig. 5_{6a}. Change of vertical displacements over time of the points in central section at the load level $\alpha = 0.6$ — detail of Fig. 5_6 (with a reduced time interval of the analysis)

Fig. 6 shows the variability of the vertical displacement over time of the selected points in the lower edge of the deep beam at different load levels $\alpha = P/P_0$. In the range of elastic capacity of the structure, the loads $\alpha = 0.1$ and $\alpha = 0.2$, (Fig. 6_1) gave the maximum deflection, just like in the *A-III* steel reinforced deep beam's span at point x_{18}, and the observed amplitude values of the vertical displacements decreased monotonously towards the support. The same behaviour of the structure was observed at the load level $\alpha = 0.3$, (Fig. 6_2), when the cracking of the concrete in proximity of the support occurred. At the load level $\alpha = 0.4$, (Fig. 6_3) and $\alpha = 0.5$, (Fig. 6_4), and similar to the *A-III* steel reinforced deep beam, the previous relation was observed: the maximum deflection was at point x_{18} of the span at lower load levels, and the observed amplitudes of vertical displacements decreased monotonously towards the support. At the load level $\alpha = 0.5$, no concrete cracks were found in the central section, unlike in the *A-III* steel reinforced deep beam. In Fig. 6_5, which shows the load level $\alpha = 0.6$, further development of the concrete cracking area is found. There was an unlimited increase of vertical displacements at the points adjacent to the span cross-section and indicative of the carrying capacity limit with a failure of the deep beam, just like in the deep beam reinforced with *A-III* steel.

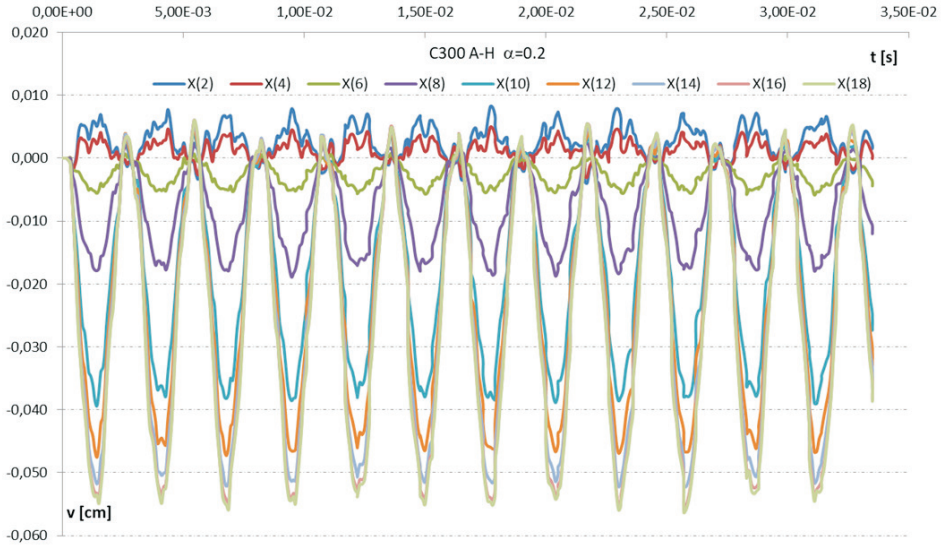

Fig. 6_1. Change of vertical displacements over time of the points in the lower edge of the deep beam at the load level $\alpha = 0.2$

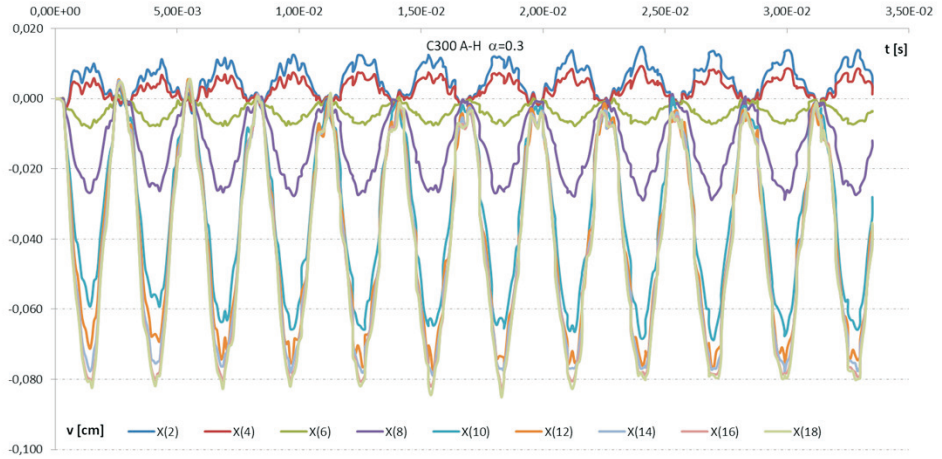

Fig. 6_2. Change of vertical displacements over time of the points in the lower edge of the deep beam at the load level $\alpha = 0.3$

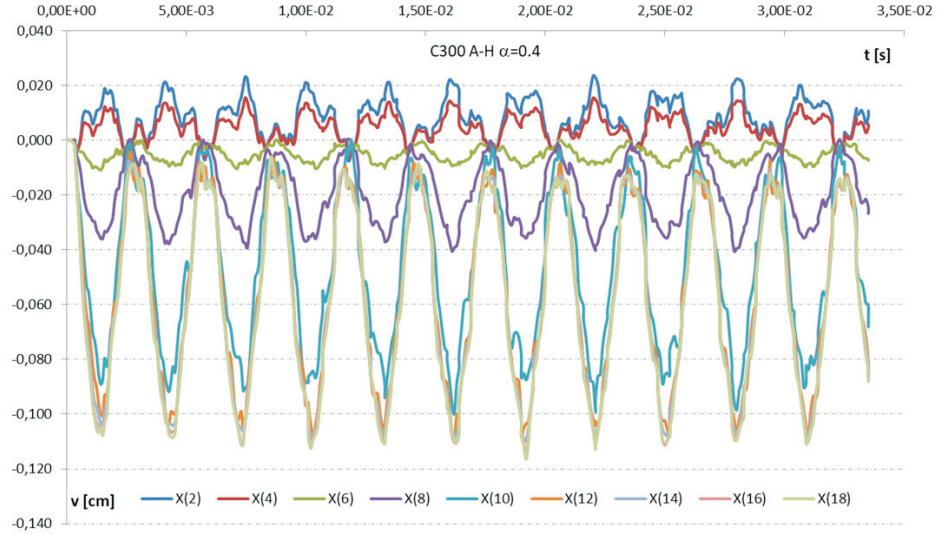

Fig. 6_3. Change of vertical displacements over time of the points in the lower edge of the deep beam at the load level $\alpha = 0.4$

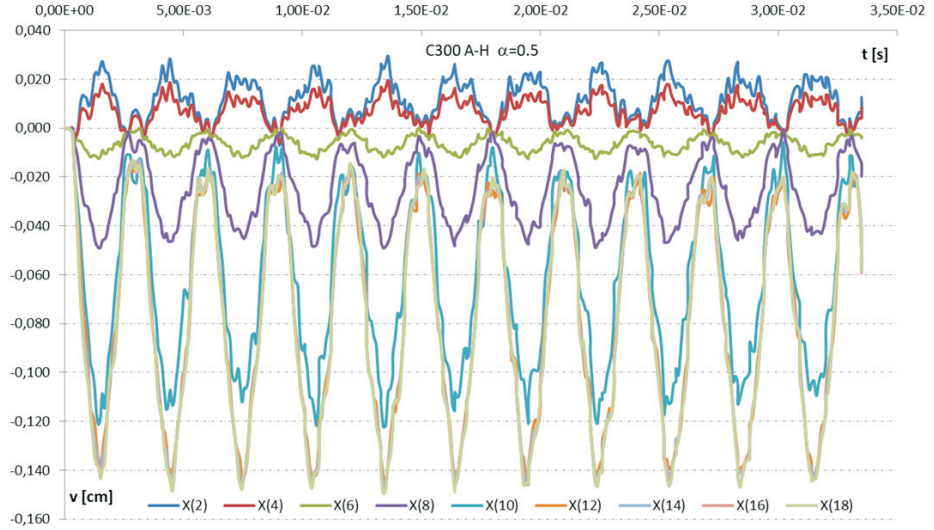

Fig. 6_4. Change of vertical displacements over time of the points in the lower edge of the deep beam at the load level $\alpha = 0.5$

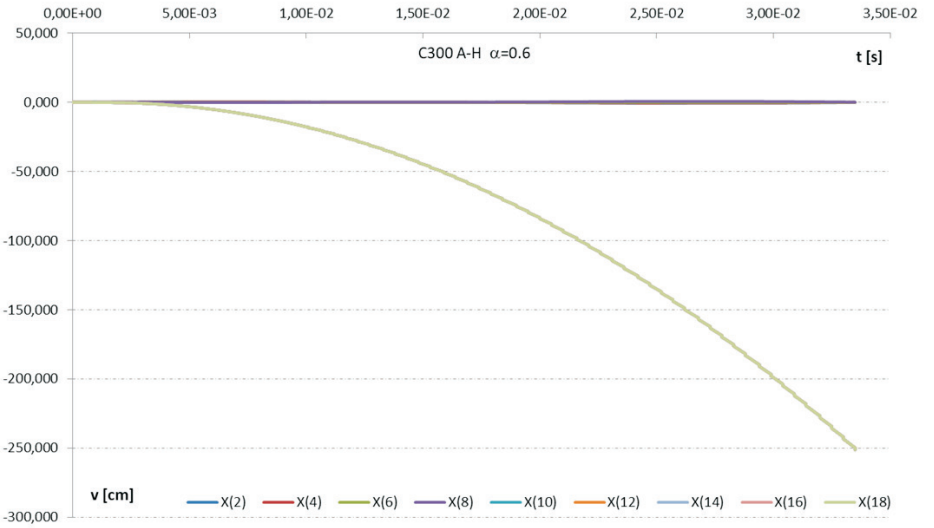

Fig. 6_5. Change of vertical displacements over time of the points in the lower edge of the deep beam at the load level $\alpha = 0.6$

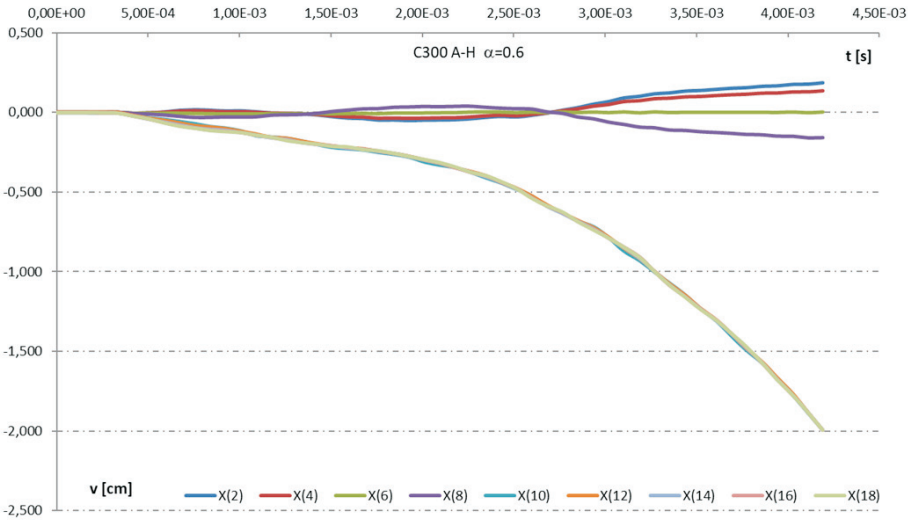

Fig. 6_{5a}. Change of vertical displacements over time of the points in the lower edge of the deep beam at the load level $\alpha = 0.6$ — detail of Fig. 6_5 (with a reduced time interval of the analysis)

Fig. 7 shows the variability of the vertical displacement over time at the selected points in the upper edge of the deep beam at different load levels $\alpha = P/P_0$. At the load levels $\alpha = 0.1$, $\alpha = 0.2$, (Fig. 7_1), $\alpha = 0.3$, (Fig. 7_2) and $\alpha = 0.4$, (Fig. 7_3), the maximum deflection was at point x_{306} of the span, just like in the deep beam reinforced with *A-III* steel, and the observed amplitude values of the vertical displacements decreased monotonously towards the support. The same behaviour of the structure, not unlike in the *A-III* steel reinforced deep beam, was observed at the load level $\alpha = 0.5$, (Fig. 7_4): there was no evidence of dynamic balance differentiation, i.e. no permanent displacement of the points on the upper edge occurred. In Fig. 7_5, which shows the load level $\alpha = 0.6$, further development of the concrete cracking area is found. There was an unlimited increase of vertical displacements at the points in the vicinity of point x_{298}, indicative of the carrying capacity limit with a failure of the deep beam. There were no significant differences in the response of the *C300* concrete deep beam between its different reinforcement steel grades, i.e. the replacement of the regular steel grade *A-III* with *A-H*.

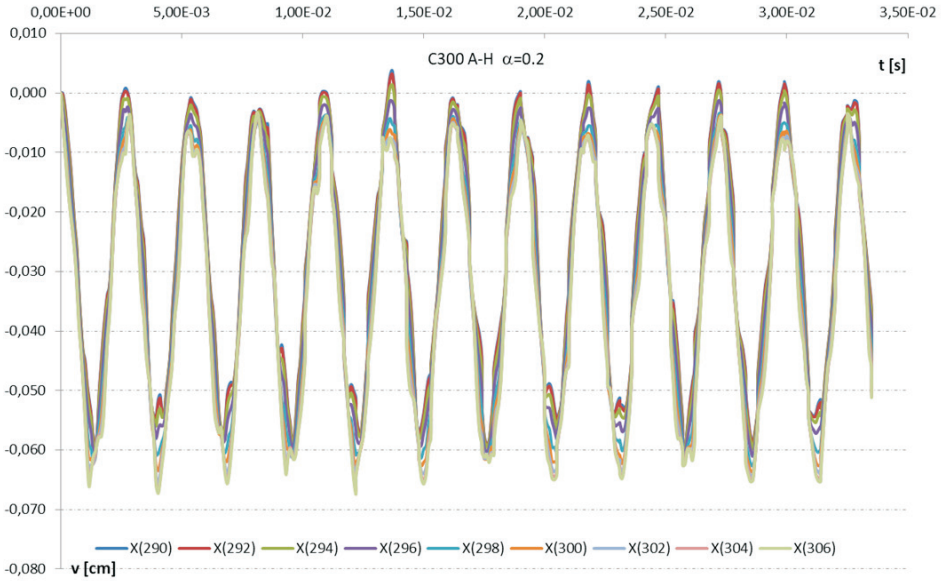

Fig. 7_1. Change of vertical displacements over time of the points in the upper edge of the deep beam at the load level $\alpha = 0.2$

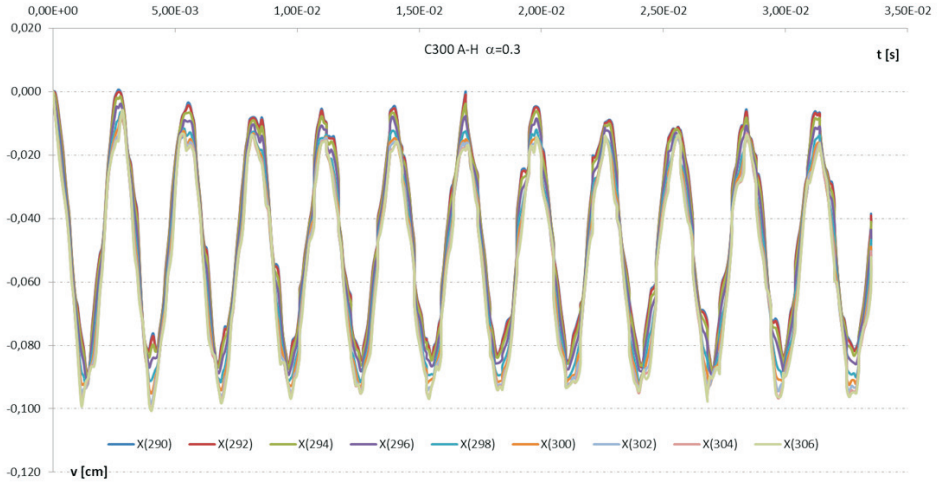

Fig. 7_2. Change of vertical displacements over time of the points in the upper edge of the deep beam at the load level $\alpha = 0.3$

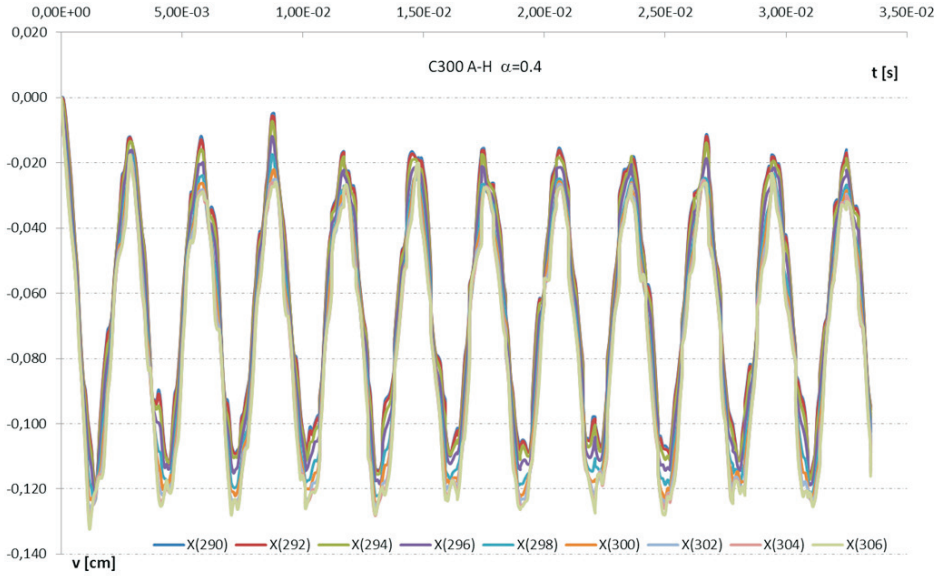

Fig. 7_3. Change of vertical displacements over time of the points in the upper edge of the deep beam at the load level $\alpha = 0.4$

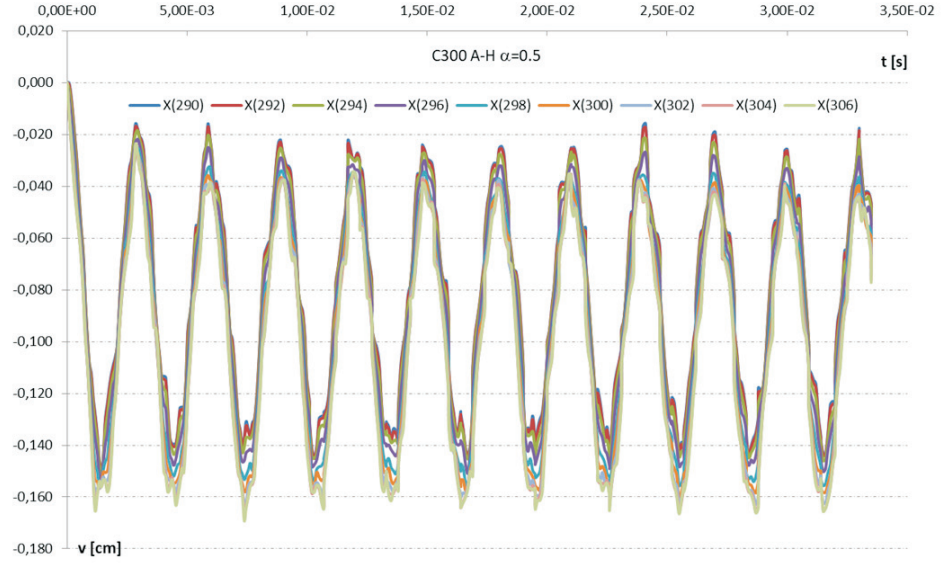

Fig. 7_4. Change of vertical displacements over time of the points in the upper edge of the deep beam at the load level $\alpha = 0.5$

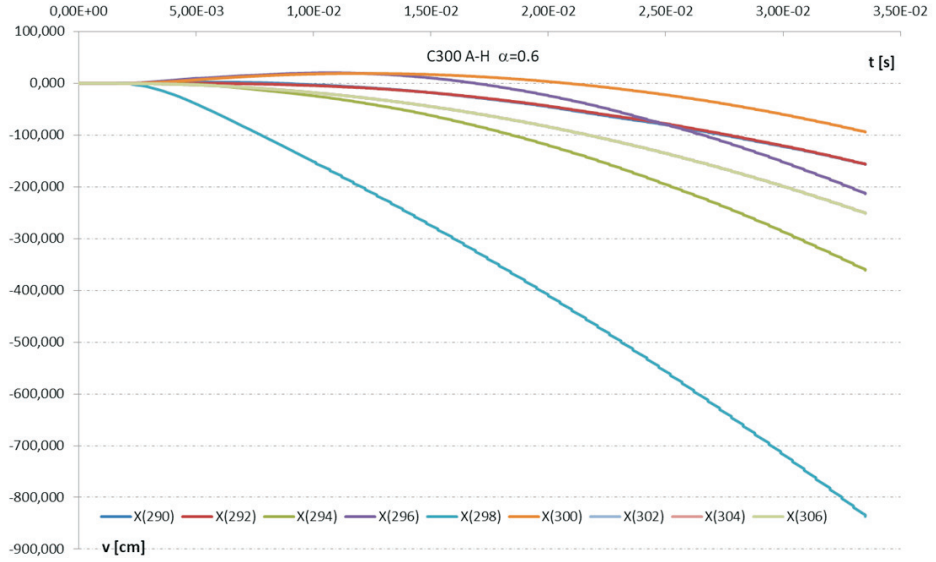

Fig. 7_5. Change of vertical displacements over time of the points in the upper edge of the deep beam at the load level $\alpha = 0.6$

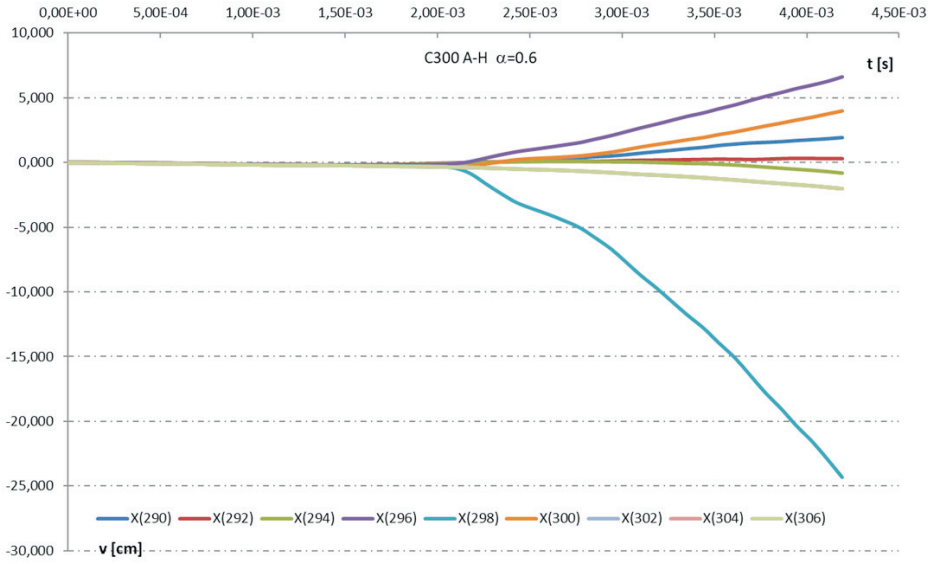

Fig. 7_{5a}. Change of vertical displacements over time of the points in the upper edge of the deep beam for load level $\alpha = 0.6$ — detail of Fig. 7_5 (with a reduced time interval of the analysis)

3. Conclusion

The work demonstrated the analysis of the displacement state of rectangular concrete deep beams made of very high strength concrete and steel of increased strength with dynamic load, including the physical nonlinearity of construction materials: concrete and reinforcing steel. A displacement dynamic state analysis of the reinforced concrete deep beam was carried out in the function of two selected parameters which defined the effort of the reinforced concrete structural element: concrete strength and steel strength. A very high-strength concrete grade *C300* was considered with two reinforcing steel grades: regular and at an increased strength. The deformation analysis of the deep beam was carried out by an observation of changes in vertical displacement of the selected points on the lower and upper edges of the deep beam and in the central section. By the analysis it was established that increasing the strength of reinforced steel can affect the mechanism of effort and failure of a concrete deep beam. The deep beam made from grade *C300* concrete and reinforced either with regular steel or the increased-strength steel revealed the propagation of crack areas not unlike in the deep beams made from grade *C200* concrete (see [11]): in the shear zone only. The deep beam reinforced with the increased-strength steel revealed an increase of the relative dynamic carrying capacity level from $\alpha = 0.5$ in the *C200* concrete deep beam to $\alpha = 0.6$ in the *C300* concrete deep beam. However, the deep beam made with grade *C300* concrete and reinforced either with the regular steel or the increased-strength steel, the same the relative dynamic carrying capacity level was found: the maximum load level was $\alpha = 0.5$.

The results provided in [10] for the reinforced concrete deep beams made from grade *C100* concrete, in [11] for the reinforced concrete deep beams made from grade *C200* concrete, and herein for the reinforced concrete deep beams made from grade *C300* concrete indicate that the mechanism of effort and failure is affected both by quantitative and qualitative changes in construction materials, i.e. concrete strength and reinforcing steel strength. The results presented confirmed it is necessary to investigate the effect of the constitutive model parameters of the very high-strength concrete and the increased-strength steel on the effort mechanism of reinforced concrete deep beams. A full evaluation of the purposefulness and effectiveness of the design engineering for deep beams with high-strength materials will require complementary numerical simulations of the deformation and stress state analysis for the concrete matrix material and the flaccid reinforcing steel bars. The results presented in this paper confirmed the correctness of the assumptions and deformation models of concrete and steel as well as the effectiveness of the methods of analysis proposed for the problems of numerical simulation of the dynamic behaviour of reinforced concrete deep beams under dynamic loads.

The work was created as a result of the research tasks carried out under the Statutory Research no. 934 at the Faculty of Civil Engineering and Geodesy of the Military University of Technology.

Received December 11, 2017. Revised February 8, 2018.

Paper translated into English and verified by company SKRIVANEK sp. z o.o., 22 Solec Street, 00-410 Warsaw, Poland.

REFERENCES

[1] Cichorski W., Stolarski A., *Metoda analizy niesprężystego zachowania tarczy żelbetowej obciążonej dynamicznie*, Biuletyn WAT, 49, 10, 2000, 5-30.

[2] Stolarski A., *Model dynamicznego odkształcania betonu*, Archiwum Inżynierii Lądowej, 37, 3-4, 1991, 405-447

[3] Cichorski W., Stolarski A., *Modelling of inelastic behaviour of reinforced concrete deep beam. Journal of Achievements in Materials and Manufacturing Engineering*, 44, 1, 2016, 37-44.

[4] Stolarski A., Cichorski W., *Influence of high strength of concrete and reinforced steel on dynamic behaviour of reinforced concrete deep beams*, Proceedings of the 12rd International Conference on Shock & Impact Loads on Structures, Singapore, 15 - 16 June 2017, 159- 168.

[5] Kleiber M., *Metoda elementów skończonych w nieliniowej mechanice kontinuum*, Warszawa, PWN, 1985.

[6] Leonhardt F., Walther R., *Wandartige träger, Report*, Deutscher Asschüb für Stahlbeton, 229, Berlin, Germany, 1966.

[7] Cichorski W., A. Stolarski A., *Analizy stanu przemieszczenia niesprężystej tarczy żelbetowej obciążonej statycznie*, Biuletyn WAT, 50, 5, 2001, 5-20.

[8] Stolarski A., Cichorski W., *Oszacowanie nośności tarczy żelbetowej z uwzględnieniem betonu bardzo wysokiej wytrzymałości*. Biuletyn WAT, 51, 2, 2002, 49-67.

[9] Cichorski W., Stolarski A., *Analizy wytężenia tarczy żelbetowej z materiałów konstrukcyjnych bardzo wysokich wytrzymałości*, Biuletyn WAT, 65, 4, 2016, 143-165.

[10] Cichorski W., *Analysis of dynamic displacement of reinforced concrete deep beams made of high strength concrete. Part 1: Analysis of dynamic displacement of a reinforced concrete deep beam made of high strength C100 grade concrete*, Biuletyn WAT, 67, 2, 2018, 111-174.

[11] Cichorski W., A*nalysis of dynamic displacement of reinforced concrete deep beams made of high strength concrete. Part 2: Analysis of dynamic displacement of a reinforced concrete deep beam made of high strength C200 grade concrete*, Biuletyn WAT, 67, 2, 2018, 27-50.

[12] Winnicki, A., Pearce, C.J., Bićanić N., *Viscoplastic Hoffman consistency model for concrete*, Comput. & Struct., 79, 2001, 7-19.

[13] Marzec I., Tejchman J., Winnicki A., *Computational simulations of concrete behaviour under dynamic conditions using elasto-visco-plastic model with non-local softening*, Computers & Concrete, 15, 4, 2015, 515-545.

W. CICHORSKI

Analiza dynamicznego przemieszczenia tarcz żelbetowych z betonu wysokiej wytrzymałości. Część III: Analiza dynamicznego przemieszczenia tarczy żelbetowej z betonu wysokiej wytrzymałości klasy C300

Streszczenie. W pracy przedstawiono analizę stanu przemieszczenia prostokątnych tarcz żelbetowych wykonanych z betonu bardzo wysokiej wytrzymałości klasy *C300* obciążonych dynamicznie z uwzględnieniem fizycznych nieliniowości materiałów konstrukcyjnych: betonu i stali zbrojeniowej. Analiza została przeprowadzona na podstawie metody zaprezentowanej w pracy [1]. Przedstawiono wyniki rozwiązań numerycznych ze szczególnym uwzględnieniem stanu przemieszczenia tarczy. Wykazano poprawność przyjętych założeń i modeli odkształcenia betonu i stali oraz efektywność metody analizy proponowanej w pracy [1] dla problemów numerycznej symulacji zachowania tarcz żelbetowych. Przeprowadzono analizę porównawczą wpływu betonu wysokiej wytrzymałości i stali podwyższonej wytrzymałości na przemieszczenia tarczy poprzez porównanie uzyskanych wyników dla tarczy z betonu *C300* z wynikami uzyskanymi dla tarczy żelbetowej wykonanej z betonu *C100* i *C200*.
Słowa kluczowe: mechanika konstrukcji, konstrukcje żelbetowe, tarcze, obciążenie dynamiczne, nieliniowość fizyczna
DOI: 10.5604/01.3001.0012.6610